The Temporal Analog of Reflection and Refraction of Optical Beams

Reflection and refraction of light at a dielectric interface and Snell's law describing them have been known for centuries and are topics discussed at length in physics textbooks.[1,2] However, their temporal analog, where an electromagnetic pulse arrives at a temporal interface, has attracted much less attention.[3,4] A temporal interface is the boundary in time separating two regions of different refractive indices. In this article we discuss "reflection" and "refraction" of optical pulses at such a temporal boundary during their propagation inside a dispersive medium. Previous works have examined temporal reflection and refraction in nondispersive media assuming that refractive index changes everywhere in the medium at a certain time.[3,4] This is analogous to examining the case of normal incidence in space. Temporal changes in the refractive index have also been studied recently in the context of adiabatic wavelength conversion.[5–11]

From a physics perspective, a spatial boundary breaks translational symmetry. As a result, the momentum of a photon can change but its energy must remain unaffected. In the case of a static temporal boundary, momentum of the photon remains unchanged but its energy must change. For this reason, a change in angle at a spatial interface translates into a change in the frequency of incident light when reflection and refraction occur at a temporal interface. We focus on optical pulses propagating inside a dispersive medium to reveal novel temporal and spectral features occurring when the pulse experiences reflection and refraction at a moving temporal boundary.

To simplify the following discussion, we assume that the optical pulse is propagating inside a waveguide with the dispersion relation $\beta(\omega)$ such that neither its polarization nor its transverse spatial shape changes during propagation. When the pulse contains multiple optical cycles, $\beta(\omega)$ can be expanded in a Taylor series around its central frequency ω_0 as[12]

$$\beta(\omega) = \beta_0 + \beta_1 (\omega - \omega_0) + \frac{\beta_2}{2} (\omega - \omega_0)^2, \tag{1}$$

where we neglect all dispersion terms higher than the second order. Physically β_1 is the inverse of the group velocity and β_2 is the group velocity dispersion (GVD). In the case of a moving temporal boundary, we work in a reference frame in which the boundary is stationary. Using the coordinate transform $t = T - z/v_{GB}$, where T is the time in the laboratory frame and v_{GB} is the velocity of the temporal boundary, the dispersion relation in the moving frame becomes

$$\beta'(\omega) = \beta_0 + \Delta\beta_1 (\omega - \omega_0) + \frac{\beta_2}{2} (\omega - \omega_0)^2 + \beta_B H (t - T_B), \tag{2}$$

where $\Delta\beta_1 = \beta_1 - 1/v_{GB}$ is a measure of a pulse's relative speed. The parameter $\beta_B = k_0 \Delta n \left(k_0 = \omega_0/c\right)$ is the magnitude of the change in the propagation constant caused by the sudden index change Δn at the temporal boundary located at $t = T_B$. The Heaviside function H $(t–T_B)$ takes a value of 0 for $t < T_B$ and 1 for $t > T_B$. For $t > T_B$, the last term in Eq. (2) shifts the dispersion curve by β_B, leading to different propagation constants in the two temporal regions. We stress that by including dispersion and allowing for a traveling boundary we have expanded on the concept of temporal reflection and refraction given in Ref. 3.

To study the impact of a temporal boundary, we write the electric field associated with the optical pulse in the form

$$E(\vec{r},t) = \hat{x} F(x,y) A(z,t) \exp(i\beta_0 z - i\omega_0 t), \tag{3}$$

where $F(x,y)$ is the transverse spatial profile and $A(z,t)$ is the slowly varying envelope of the pulse. Use of Maxwell's equations together with the dispersion relation in Eq. (2) then leads to the following time-domain equation:[12]

$$\frac{\partial A}{\partial z} + \Delta\beta_1 \frac{\partial A}{\partial t} + i \frac{\beta_2}{2} \frac{\partial^2 A}{\partial t^2} = i\beta_B H (t - T_B) A. \tag{4}$$

For numerical purposes we normalize this equation using

$$\tau = \frac{t}{T_0}, \quad \xi = \frac{z}{L_D}, \quad A(z,t) = \sqrt{P_0}\, U(\xi,\tau), \tag{5}$$

where T_0 is the width, P_0 is the peak power of the incident pulse, and $L_D = T_0^2 / |\beta_2|$ is the dispersion length. The normalized amplitude $U(\xi,\tau)$ satisfies

$$\frac{\partial U}{\partial \xi} + d\,\frac{\partial U}{\partial \tau} + b_2\,\frac{i}{2}\,\frac{\partial^2 U}{\partial \tau^2} = i\beta_B L_D H(\tau - \tau_B)\,U\,. \tag{6}$$

where $d = \Delta\beta_1 L_D / T_0$, $\tau_B = T_B / T_0$, and $b_2 = \pm 1$ depending on the sign of β_2.

We solved Eq. (6) numerically with the standard split-step Fourier method,[12] assuming a Gaussian shape of input pulses. For the numerical simulations that follow, the temporal boundary was located at $\tau_B = 5$ and the dispersion was taken to be normal ($b_2 = +1$). We chose $d = 20$ to ensure that the center of the optical pulse would cross the boundary halfway through the total propagation length of $\xi = 0.5$.

As a first example of temporal reflection and refraction, Fig. 143.39 shows (a) temporal and (b) spectral evolutions of a Gaussian input pulse for $\beta_B L_D = 100$. The temporal evolution in part (a) is strikingly similar to an optical beam hitting a spatial boundary. From Fig. 143.39(a) we see that the trailing edge of the pulse reaches the boundary near $\xi = 0.15$ as the faster temporal boundary begins to overtake the optical pulse. Although most of pulse energy is transmitted across the boundary, the pulse "bends" toward it and its speed changes. The transmitted pulse is also narrower in time, similar to how a refracted optical beam becomes narrower in space when it is bent toward the spatial interface. A small part of pulse energy is "reflected" and begins traveling away from the temporal boundary. This reflected pulse has the same temporal width but its speed increases considerably. In this case both the energy and momentum of a photon must change simultaneously while crossing the boundary.

Figure 143.39(b) shows how temporal changes are accompanied by a multitude of spectral changes. In particular, notice how the spectrum shifts and splits as the pulse crosses the temporal boundary. Recall that the temporal analog of an angle is the frequency. From a fundamental perspective, spectral changes occur because a temporal boundary breaks symmetry in time. As a result, photon momentum in the moving frame (or β') must be conserved while photon energy (or ω) may change. This suggests that the dispersion relation in Eq. (2) should be able to explain all spectral changes. Figure 143.40 shows dispersion curves for $\tau < \tau_B$ (dashed blue) and $\tau > \tau_B$ (solid green). In the moving frame, the slope of these curves gives the speed of the pulse relative to the temporal boundary,

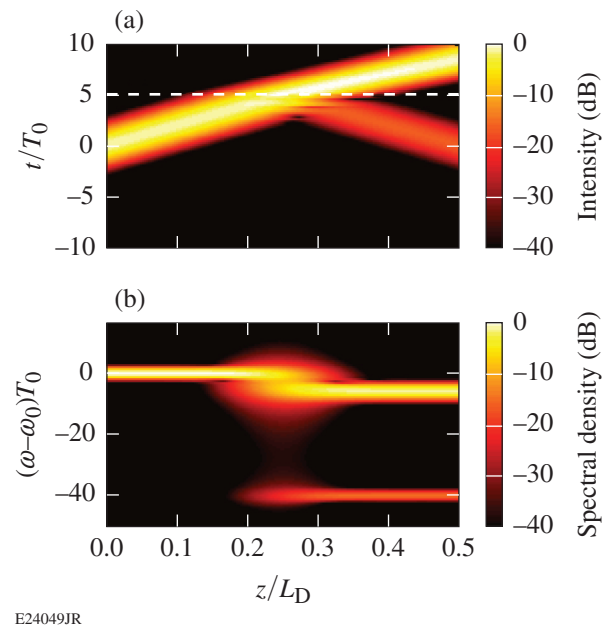

Figure 143.39
Evolution of (a) the pulse shape and (b) the spectrum in the presence of a temporal boundary at $\tau_B = 5$ (dashed white line) with $\beta_B L_D = 100$. Time is measured in a reference frame that moves with the temporal boundary.

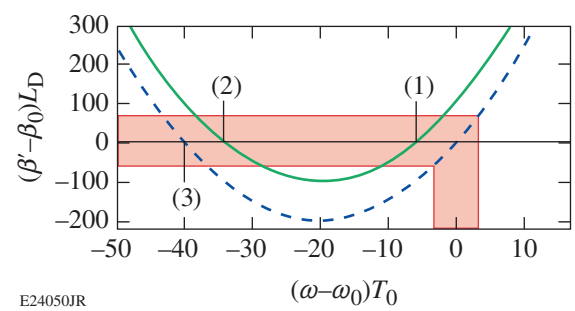

Figure 143.40
Normalized dispersion curves for $\tau < \tau_B$ (dashed blue) and $\tau > \tau_B$ (solid green). The shaded region shows the spectral extent of the input pulse and the corresponding range of propagation constants for $\tau < \tau_B$. The slope of the dispersion curve is related to the speed of the pulse relative to the traveling temporal boundary.

rather than the actual group velocity. As mentioned earlier, even though β (related to photon momentum) is not conserved, the corresponding quantity β' is conserved in the moving frame. We use this conservation law to understand the spectral shifts of refracted and reflected pulses.

To conserve β' when transitioning from the $\tau < \tau_B$ region to the $\tau > \tau_B$ region, each frequency component must shift from the dashed curve to a point on the solid curve with the same value of β'. Because the curve is locally parabolic, the two frequencies at points (1) and (2) on the solid curve match the initial value of β'. Only point (1) is a valid solution, however, since the slope, related to the speed of the pulse, should have the same sign for the transmitted pulse. The entire pulse spectrum shifts toward the red side (for $\beta_B > 0$) since each frequency component of the pulse must shift accordingly. Since the slope of the dispersion curve at the new central frequency is different, the transmitted pulse must travel at a different speed relative to the temporal boundary. This change in the group velocity is what leads to the apparent bending observed in Fig. 143.39(a).

The reflected pulse is caused by the second point on the dashed curve that has the same propagation constant, marked as point (3) in Fig. 143.40. This point must have the opposite slope to ensure that the pulse reflects back into the $\tau < \tau_B$ region. We stress that the reflected pulse does not travel backward in time or space; rather its speed is increased so much that it moves away from the temporal boundary. Both the reflected pulse and the temporal boundary continue to propagate through the dispersive medium in the $+z$ direction. Figure 143.39(b) shows that the spectrum of the reflected pulse is shifted toward the red side by about $\Delta\nu = 40/(2\pi T_0)$ or by more than 6 THz for a pulse with $T_0 = 1$ ps. It also shows that the energy transfer occurs over a relatively small distance during which the pulse passes through the temporal boundary.

So far we have considered only the central frequency of the optical pulse. However, the pulse has a finite spectral width and β' must be conserved for all frequencies in the spectrum. In Fig. 143.40, the shaded region shows the width of the input pulse spectrum and the corresponding range of propagation constants for $\tau < \tau_B$. We can see that the shaded region on the transmitted curve covers a much wider spectral region than on the incident curve. This leads to the spectral broadening and temporal narrowing of the refracted pulse. If the sign of β_B was reversed, shifting the curve in the opposite direction, the pulse spectrum would be compressed and the pulse would correspondingly broaden in time.

One may ask how much the momentum changes in the laboratory frame. It is easy to see that $\beta = \beta' + (\omega - \omega_0)/v_{GB}$. Since β' remains constant, β changes by an amount $(\omega - \omega_0)/v_{GB}$. Clearly, a moving boundary breaks both temporal and spatial symmetries, forcing momentum and energy to change simultaneously. This is similar to the behavior observed in interband photonic transitions.[13]

To obtain analytic expressions for the spectral shifts caused during temporal reflection and refraction, we impose the requirement of momentum conservation in the dispersion relation given in Eq. (2). To do so, we choose a specific frequency component, i.e., the center frequency ω_0, and set $\beta'(\omega) = \beta_0$ in Eq. (2), resulting in the quadratic equation

$$\frac{\beta_2}{2}(\omega - \omega_0)^2 + \Delta\beta_1(\omega - \omega_0) + \beta_B H(t - T_B) = 0. \quad (7)$$

The last term vanishes for $t > T_B$ and the two solutions of the quadratic equation are

$$\omega_i = \omega_0 \quad \text{and} \quad \omega_r = \omega_0 - 2\left(\Delta\beta_1/\beta_2\right). \quad (8)$$

These solutions represent the incident and reflected frequencies and correspond to the points (1) and (3), respectively, in Fig. 143.40. The transmitted frequency is found by noting that the last term in Eq. (7) is finite for $t > T_B$ and has the value β_B. Solving the quadratic equation again, we obtain

$$\omega_t = \omega_i + \frac{\Delta\beta_1}{\beta_2}\left[-1 \pm \sqrt{1 - \frac{2\beta_B\beta_2}{(\Delta\beta_1)^2}}\right]. \quad (9)$$

As discussed earlier, only the positive sign corresponds to a physical solution shown as point (2) in Fig. 143.40. In the limit $\Delta\beta_1 \gg \sqrt{\beta_B\beta_2}$, this equation can be approximated as

$$\omega_t = \omega_i - \frac{\beta_B}{\Delta\beta_1} = \omega_i - \frac{k_0\Delta n}{\Delta\beta_1}. \quad (10)$$

The numerical results shown in Fig. 143.39 agree with these analytic expressions derived using the concept of momentum conservation.

The analytical results found in this article provide considerable insight into the phenomena of temporal reflection and refraction of optical pulses. Consider first the frequency shift of the reflected pulse: Eq. (8) indicates that this shift depends

on both the sign and magnitude of the GVD governed by the parameter β_2. In particular, it disappears as $\beta_2 \to 0$. It follows from Eq. (2) that the parabolic dispersion curve seen in Fig. 143.40 reduces to a straight line in this limit, indicating that point (3) in Fig. 143.40 ceases to exist. Note also that the direction of frequency shifts depends on the nature of GVD. A red shift occurring for normal dispersion becomes a blue shift in the case of anomalous dispersion. Another noteworthy feature is that the frequency shifts do not depend on the refractive index change Δn across the temporal boundary. Of course, the energy transferred to the reflected pulse depends strongly on the magnitude of β_B. These features are analogous to what occurs at a spatial interface.

We now ask how large the spectral shift can be for the reflected pulse. As discussed earlier, a spectral shift of about 6 THz occurs for the parameters used in Fig. 143.39. Equation (8) indicates that even larger spectral shifts are possible by reducing the magnitude of the GVD parameter; i.e., by operating close to the zero-dispersion wavelength of the waveguide used to observe this phenomenon.

The refracted pulse also undergoes a spectral shift that is analogous to a change in the direction of an optical beam refracted at a spatial boundary. As seen in Eq. (9), this shift depends on the magnitude of β_B, in addition to the GVD parameter β_2 and the differential group delay (DGD) $\Delta\beta_1$ of the pulse. In the limit $\Delta\beta_1 \gg \sqrt{\beta_B \beta_2}$, the spectral shift becomes independent of β_2. Its magnitude in all cases is much smaller than that found for the reflected pulse. As an example, for an index change of $\Delta n = 10^{-4}$ and $\Delta\beta_1 = 100$ ps/m, this shift is about 1 THz at a wavelength of 1.06 μm.

Although Eqs. (8) and (9) provide the expected frequency shifts, they do not have an obvious resemblence to the spatial laws of reflection and refraction. Indeed, it is difficult to find analogous relations since the concept of an angle, familiar in the spatial context, is replaced with the DGD $\Delta\beta_1$, indicating the speed of the pulse relative to a temporal boundary. Nevertheless, one may gain some insight if we use the location of extremum of the dispersion curve in Fig. 143.40 as a reference frequency ω_c, where the slope $d\beta/d\omega = 0$. If we shift the origin in Fig. 143.40 so that all frequencies are measured from the reference frequency $\omega_c = \omega_0 - \Delta\beta_1 / \beta_2$ and use the notation $\Delta\omega = \omega - \omega_c$, the reflected and transmitted frequencies are related to the input frequency as

$$\Delta\omega_r = -\Delta\omega_i, \qquad \Delta\omega_t = \Delta\omega_i \sqrt{1 - \frac{2\beta_B \beta_2}{(\Delta\beta_1)^2}}. \tag{11}$$

The first equation is analogous to the law of reflection. The second one can be written in the following suggestive form:

$$\Delta\omega_t = \Delta\omega_i \cos\alpha, \qquad \sin\alpha = \sqrt{\frac{2\beta_B \beta_2}{(\Delta\beta_1)^2}}. \tag{12}$$

For small values of β_B, α remains relatively small, resulting in small frequency shifts during refraction and small changes in the pulse speed. Frequency shifts increase with increasing β_B. At some value of parameters, α becomes $\pi/2$ and $\Delta\omega_t$ vanishes. At that point, the transmitted pulse's central frequency coincides with the frequency ω_c.

We must ask what happens if β_B is large enough that α loses its meaning. Since $\Delta\omega_t$ becomes undefined, no refracted pulse can form past the temporal boundary and the incident pulse must be totally reflected. This is the temporal analog of the well-known phenomenon of total internal reflection (TIR). The condition for the temporal TIR is found from Eq. (12) to be

$$\sqrt{2\beta_B \beta_2} > \Delta\beta_1. \tag{13}$$

Temporal TIR can also be understood from the two dispersion curves shown in Fig. 143.40. When β_B is large enough to shift the green curve in Fig. 143.40 completely out of the shaded region, momentum conservation or phase matching cannot be achieved for any spectral component of the incident pulse. As a result, no pulse energy can enter the $\tau > \tau_B$ region beyond the temporal boundary; however, the momentum can still be conserved for the reflected pulse. As a result, the pulse should be completely reflected at the boundary. We performed numerical simulations to confirm that this is indeed the case. Figure 143.41 shows the numerical results for $\beta_B L_D = 280$, a value that places the transmitted curve just above the shaded region. As predicted by our simple theory, there is no transmitted pulse and the entire pulse is reflected. The spectral evolution in Fig. 143.41(b) shows how the pulse energy is transferred to the reflected pulse over a small distance after the trailing end of the incident pulse hits the temporal boundary. Closer inspection reveals that a portion of the pulse extends past the temporal boundary, forming a temporal analog to the evanescent wave.

The existence of temporal TIR seems to contradict the findings in Ref. 3, where a temporal analog of Snell's law is derived that does not allow for TIR to occur. However, the study in Ref. 3 did not include the effects of dispersion. Indeed, our theory shows that no reflection occurs if β_2 is set to 0.

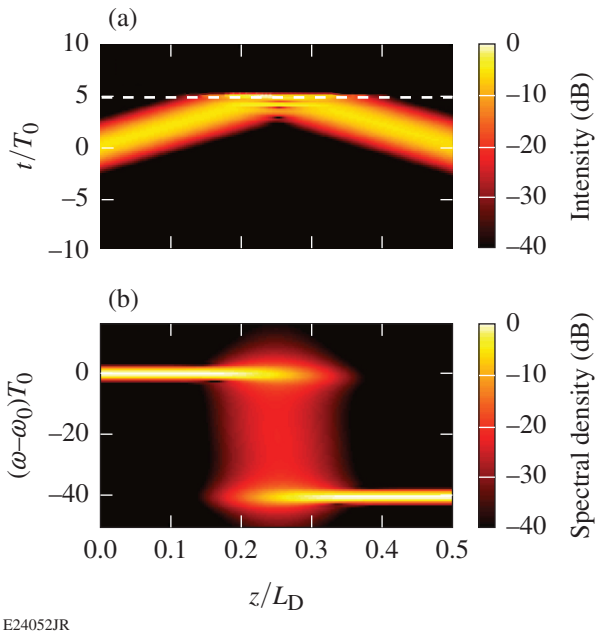

Figure 143.41
(a) Temporal and (b) spectral evolutions of an optical pulse undergoing total internal reflection (TIR) at a temporal boundary located at $\tau_B = 5$ (dashed white line). The index change is large enough that $\beta_B L_D = 280$. Time is measured in a reference frame that moves with the temporal boundary.

In summary, we have shown that when an optical pulse approaches a moving temporal boundary across which the refractive index changes, it undergoes a temporal equivalent of reflection and refraction of optical beams at a spatial boundary. The main difference is that the role of angle is played by changes in the frequency. The dispersion curve of the material in which the pulse is propagating plays a fundamental role in determining the frequency shifts experienced by the reflected and refracted pulses. The analytic expressions that we were able to obtain for these two frequency shifts show that the spectral shift is relatively small for the refracted pulse but can be quite large for the reflected pulse. Moreover, the shifts can be either on the red side or on the blue side of the spectrum of the incident pulse, depending on the nature of both the group-velocity dispersion and the refractive index change. These spectral shifts are caused by a transfer of energy between the pulse and the temporal boundary while the number of photons is conserved.[3] Because our temporal boundary is induced by an external source, this is not a closed system and energy is not conserved in the pulse. We have also indicated the conditions under which an optical pulse experiences the temporal analog of TIR. Numerical results confirm all analytical predictions based on the physical concept of momentum conservation in the moving frame.

An experimental observation of reflection, refraction, and TIR at a temporal boundary will be of immense interest. Our estimates show that changes in the refractive index across this boundary can be as small as 10^{-6} for verifying our theoretical and numerical predictions. The main issue is how to control the relative speed of the pulse with respect to the temporal boundary. One possibility is to use a traveling-wave electro-optic modulator in which a microwave signal propagates at a different speed than that of the optical pulse. A pump–probe configuration in which cross-phase modulation would be used to produce a moving temporal boundary may also be possible but will require pump pulses of high energies.

ACKNOWLEDGMENT

This material is based upon work supported by the Department of Energy National Nuclear Security Administration under Award Number DE-NA0001944, the University of Rochester, and the New York State Energy Research and Development Authority. The support of DOE does not constitute an endorsement by DOE of the views expressed in this article.

REFERENCES

1. M. Born and E. Wolf, *Principles of Optics: Electromagnetic Theory of Propagation, Interference, and Diffraction of Light*, 7th expanded ed. (Cambridge University Press, Cambridge, England, 1999), pp. 752–758.
2. B. E. A. Saleh and M. C. Teich, *Fundamentals of Photonics*, 2nd ed. (Wiley-Interscience, Hoboken, NJ, 2007).
3. J. T. Mendonça and P. K. Shukla, Phys. Scr. **65**, 160 (2002).
4. Y. Xiao, D. N. Maywar, and G. P. Agrawal, Opt. Lett. **39**, 574 (2014).
5. M. F. Yanik and S. Fan, Phys. Rev. Lett. **93**, 173903 (2004).
6. M. Notomi and S. Mitsugi, Phys. Rev. A **73**, 051803(R) (2006).
7. S. F. Preble, Q. Xu, and M. Lipson, Nat. Photonics **1**, 293 (2007).
8. T. Tanabe *et al.*, Phys. Rev. Lett. **102**, 043907 (2009).
9. T. Kampfrath *et al.*, Opt. Lett. **34**, 3418 (2009).
10. T. Kampfrath *et al.*, Phys. Rev. A **81**, 043837 (2010).
11. A. Nishida *et al.*, Appl. Phys. Lett. **101**, 161118 (2012).
12. G. P. Agrawal, *Nonlinear Fiber Optics*, 5th ed. (Academic Press, Boston, 2013).
13. M. Castellanos Muñoz *et al.*, Phys. Rev. Lett. **112**, 053904 (2014).